

QUASI-3D NEARSHORE CURRENT MODELLING: WAVE-INDUCED SECONDARY CURRENT

M.J.F. Stive and H.J. de Vriend*

ABSTRACT

A profile function technique combined with a horizontally two-dimensional current formulation has recently been suggested to describe the three-dimensional current system in the coastal zone (De Vriend and Stive, 1987). In this quasi three-dimensional approach the current is divided into a primary component, due to the vertically uniform part of the driving forces, and a secondary component, due to the vertical non-uniformity of the driving forces. The wave-induced secondary current was evaluated using a three layer concept, in which the effects of the wave boundary layer are disregarded for the breaking wave fraction. The validity of this simplification and the implications for the quasi-3D formulation are investigated by integrating the boundary layer treatment of Svendsen et al. (1987) into the three layer concept.

1. INTRODUCTION

The nearshore current system and the associated sediment transport field are spatially of a three-dimensional nature. In nearly all nearshore wave-current-morphology models the vertical dimension is only accounted for in situations where the processes are uniform in one of the horizontal dimensions. Models which deal with nonuniformity in two horizontal dimensions are traditionally depth-integrated. In general, however, three-dimensionality is present, with the variations in the two horizontal dimensions of the same order of magnitude and the vertical variation much stronger. In that case, profile techniques can be very useful. In 2DH wave modelling, for instance, it is common practice to write the wave potential as the product of a vertical profile function and a depth-invariant quantity that is actually solved by the model (cf. Berkhoff, 1976). Velocity profile techniques have proved quite useful to describe three-dimensional nearly-horizontal flows in shallow water (Davies, 1980; De Vriend, 1981). Making use of this "quasi-3D" modelling technique, De Vriend and Stive (1986) -denoted as DVS in the following- give a first formulation for a quasi-3D nearshore current model.

Starting from the complete 3D Reynolds equations, integrated over the waves, and a gradient-type turbulence closure with a scalar turbulence viscosity, similarity hypotheses are made for all dependent variables and the turbulence viscosity. This provides the possibility to distinguish between the primary and the secondary flow, with the former defined as the flow in the direction of the depth-averaged velocity and having the vertical distribution that corresponds with a vertically uniform driving force (e.g. a hydrostatic pressure gradient).

* Delft Hydraulics. P.O. Box 152, 8300 AD Emmeloord, The Netherlands

All other flow components are called secondary. If the turbulence viscosity is given a vertical distribution and its depth-average is related to current and wave properties, the primary flow velocity and the associated bottom shear stress can be determined.

This separation procedure yields a primary flow model, consisting of a profile function, a bottom shear stress relationship and the conventional depth-integrated equations. Besides, it yields equations for the secondary flow due to curvature of the primary flow, the coriolis-effect, wind and wave action.

Of the several secondary flow sources, only the one originating from the wave motion was taken into account in the DVS-model. This is, however, justified if the attention is focussed on the surf zone of a nearly uniform coast, although the formulations as such are so general, that they allow for more complex situations.

To derive the wave-induced secondary flow, DVS divide the water column into three layers, viz. a surface layer above the wave trough level, a middle layer and a bottom layer. The surface layer model is reduced to the formulation of the effective shear stress and the mass flux. For breaking waves a zero bottom shear stress is shown to lead to acceptable predictions of the current outside the wave boundary layer. This means that for this part of the current the bottom layer as such was left out of consideration. Thus, DVS reduced the problem to solving the velocity in the middle layer from the horizontal momentum balance.

This treatment of the wave boundary layer flow is - although practical and shown to yield good results - not consistent in a breaking wave situation. Recently, Svendsen et al. (1987) proposed a model of the boundary layer flow under breaking waves which uses a patching technique for the secondary current and the associated shear stress between the bottom layer and the middle layer. The relevance of this approach for the quasi-3D model is evaluated in the present paper.

2. THE QUASI-3D CURRENT MODEL

We consider the nearly horizontal flow, averaged over the oscillatory wave and turbulent motion, in a 3D coastal region.

If, apart from the wave-induced orbital motion, the current involves no strong vertical accelerations, the time-mean pressure can be approximated by

$$p \approx p_h - \rho \langle \tilde{w}^2 \rangle \quad (1)$$

in which: p = pressure,
 p_h = hydrostatic pressure,
 ρ = mass density of the fluid,
 \tilde{w} = vertical component of the wave orbital velocity,
 $\langle \dots \rangle$ = average over the waves.

If, in addition, the Boussinesq-hypothesis is adopted to model the Reynolds stress terms, the wave- and turbulence-averaged horizontal momentum equations can be written as

$$\frac{\partial u}{\partial t} + u \frac{\partial u}{\partial x} + v \frac{\partial u}{\partial y} + w \frac{\partial u}{\partial z} - f_c v = -\frac{1}{\rho} \frac{\partial p_n}{\partial x} + \frac{\partial}{\partial x} (v_t \frac{\partial u}{\partial x}) + \frac{\partial}{\partial y} (v_t \frac{\partial u}{\partial y}) + \frac{\partial}{\partial z} (v_t \frac{\partial u}{\partial z}) - \frac{\partial}{\partial x} (\langle \tilde{u}^2 \rangle - \langle \tilde{w}^2 \rangle) - \frac{\partial}{\partial y} (\langle \tilde{u}\tilde{v} \rangle) - \frac{\partial}{\partial z} (\langle \tilde{u}\tilde{w} \rangle) \quad (2)$$

$$\frac{\partial v}{\partial t} + u \frac{\partial v}{\partial x} + v \frac{\partial v}{\partial y} + w \frac{\partial v}{\partial z} + f_c u = -\frac{1}{\rho} \frac{\partial p_n}{\partial y} + \frac{\partial}{\partial x} (v_t \frac{\partial v}{\partial x}) + \frac{\partial}{\partial y} (v_t \frac{\partial v}{\partial y}) + \frac{\partial}{\partial z} (v_t \frac{\partial v}{\partial z}) - \frac{\partial}{\partial x} (\langle \tilde{u}\tilde{v} \rangle) - \frac{\partial}{\partial y} (\langle \tilde{v}^2 \rangle - \langle \tilde{w}^2 \rangle) - \frac{\partial}{\partial z} (\langle \tilde{v}\tilde{w} \rangle) \quad (3)$$

with: x, y = horizontal co-ordinates in a cartesian system,
 z = vertical co-ordinate in this system,
 u, v, w = wave- and turbulence-mean velocity components,
 p_n = $p_h + \rho g(z - \langle z_B \rangle)$ = total hydrostatic pressure,
 f_c = coriolis coefficient
 g = acceleration due to gravity,
 $\langle z_B \rangle$ = mean water level,
 v_t = turbulence viscosity (eddy viscosity),
 \tilde{u}, \tilde{v} = horizontal components of the wave orbital velocity.

Together with the corresponding equation of continuity

$$\frac{\partial u}{\partial x} + \frac{\partial v}{\partial y} + \frac{\partial w}{\partial z} = 0 \quad (4)$$

these equations describe the wave- and turbulence-averaged current, which may still be time-dependent on a time-scale much larger than the wave period or the time-scale of turbulence.

Equations (2) and (3) include the assumption that turbulence and wave motion are uncorrelated.

Furthermore, outside the bottom boundary layer, the last term in either momentum equation is neglected with regard to the corresponding Reynolds stress term, since the horizontal and vertical velocity components of the orbital velocity are approximately 90 degrees out of phase, whereas the turbulent velocity components are much less so.

Similarity approach

The basic idea of the current model is a similarity approach, assuming that each dependent variable can be written in the form

$$u = \sum_i \bar{u}_i(x, y, t) f_i \left(\frac{z - z_b}{h} \right) \quad (5)$$

in which z_b denotes the bottom level and h the water depth for $z_B = \langle z_B \rangle$. The quantity \bar{u}_i is independent of z and the vertical distribution function f_i is invariant, or at most weakly varying, with x and y .

If the series in (5) would be extended to an infinite number of terms, this approach would correspond with the formal separation of variables. In the present model, it is attempted to define the constituents in such a way, that a truncated series of only a few terms yields a good approximation of the solution.

The dependent variables in the current model are the pressure p_n (or the mean water surface elevation $\langle z_s \rangle$), and the velocity components u , v and w . Besides, the system requires a turbulence closure, relating v_t to the velocity field.

The series (5) for the total hydrostatic pressure simply reduces to

$$p_n = p_n(x, y, t) \quad (6)$$

which reflects the assumption of hydrostaticity.

The current is split into what will be called a "primary" and a "secondary" current, according to the definition:

$$u = u_p + u_s \quad \text{with } u_p = \bar{u}(x, y, t) f_p \left(\frac{z-z_b}{h} \right) \quad \text{and } \bar{u}_s = 0 \quad (7)$$

$$v = v_p + v_s \quad \text{with } v_p = \bar{v}(x, y, t) f_p \left(\frac{z-z_b}{h} \right) \quad \text{and } \bar{v}_s = 0 \quad (8)$$

in which the suffix p denotes the primary current, the suffix s the secondary current and the overbar the depth-averaged value. So, by definition, the depth-averaged flow is determined entirely by the primary current.

It has to be noted that the definitions (7) and (8) are not unique, as long as the vertical distribution function f_p is not specified. Besides, u_s and v_s remain to be written as a similarity series like (5). These points will be considered furtheron.

Once the horizontal components of the primary and the secondary flow velocity have been defined, the vertical components follow from the equation of continuity (4):

$$\frac{\partial w_p}{\partial z} = - \frac{\partial u_p}{\partial x} - \frac{\partial v_p}{\partial y} \quad \text{and} \quad \frac{\partial w_s}{\partial z} = - \frac{\partial u_s}{\partial x} - \frac{\partial v_s}{\partial y} \quad (9)$$

For simplicity, an algebraic turbulence closure is adopted, relating v_t algebraically to the local flow velocity. Besides, v_t is assumed to be described by the one-term similarity "series"

$$v_t = \bar{v}_t(x, y, t) \phi \left(\frac{z-z_b}{h} \right) \quad (10)$$

in which the depth-average \bar{v}_t and the vertical distribution function ϕ remain to be specified.

Turbulence model

The Boussinesq hypothesis combined with an algebraic relationship between the turbulence viscosity and the flow velocity has often been applied with success in models of large-scale steady or slowly varying flow in shallow water. Also DVS rely on this approach. They adopt the traditional steady current distribution and adapt it to the effects of the oscillatory wave motion on the bottom layer and of the breaking wave induced turbulent motion on the upper layer. The depth average value is determined by the current and the breaking wave dissipation. Here, we rely on a simpler formulation which is discussed furtheron.

Division of the flow equations

Substitution of the definitions (7) and (8) into the x-momentum equation (2) yields

$$\begin{aligned} & \frac{\partial u}{\partial t} + u_p \frac{\partial u_p}{\partial x} + v_p \frac{\partial u_p}{\partial y} + w_p \frac{\partial u_p}{\partial z} - f_c v_p + \frac{\partial u_s}{\partial t} + u_s \frac{\partial u_s}{\partial x} + v_s \frac{\partial u_s}{\partial y} + w_s \frac{\partial u_s}{\partial z} \\ & - f_c v_s + u_s \frac{\partial u_p}{\partial x} + v_s \frac{\partial u_p}{\partial y} + w_s \frac{\partial u_p}{\partial z} + u_p \frac{\partial u_s}{\partial x} + v_p \frac{\partial u_s}{\partial y} + w_p \frac{\partial u_s}{\partial z} = - \frac{1}{\rho} \frac{\partial p_n}{\partial x} + \\ & + \frac{\partial}{\partial x} (v_t \frac{\partial u_p}{\partial x}) + \frac{\partial}{\partial y} (v_t \frac{\partial u_p}{\partial y}) + \frac{\partial}{\partial z} (v_t \frac{\partial u_p}{\partial z}) + \frac{\partial}{\partial x} (v_t \frac{\partial u_s}{\partial x}) + \frac{\partial}{\partial y} (v_t \frac{\partial u_s}{\partial y}) + \\ & + \frac{\partial}{\partial z} (v_t \frac{\partial u_s}{\partial z}) - \frac{\partial}{\partial x} (\langle \tilde{u}^2 \rangle - \langle \tilde{w}^2 \rangle) - \frac{\partial}{\partial y} (\langle \tilde{u}\tilde{v} \rangle) \end{aligned} \quad (11)$$

Substitution into the y-momentum equation (3) yields a similar result. Integration of eq. (11) from the bottom to a point above the highest water surface elevation yields, after some elaboration:

$$\begin{aligned} & \frac{\partial \bar{u}}{\partial t} + \frac{f^2}{p} (\bar{u} \frac{\partial \bar{u}}{\partial x} + \bar{v} \frac{\partial \bar{u}}{\partial y}) - f_c \bar{v} + \frac{1}{h} [\frac{\partial}{\partial x} (\bar{u}^2) + \frac{\partial}{\partial y} (\bar{u}_s \bar{v}_s)] + \\ & + \frac{1}{h} [\frac{\partial}{\partial x} (\bar{u}_p \bar{u}_s) + \frac{\partial}{\partial y} (\bar{u}_p \bar{v}_s)] + \frac{1}{h} [\frac{\partial}{\partial x} (\bar{u}_s \bar{u}_p) + \frac{\partial}{\partial y} (\bar{u}_s \bar{v}_p)] = - \frac{1}{\rho} \frac{\partial p_n}{\partial x} + \\ & + \frac{\partial}{\partial x} (v_t \frac{\partial u_p}{\partial x}) + \frac{\partial}{\partial y} (v_t \frac{\partial u_p}{\partial y}) + \frac{\partial}{\partial x} (v_t \frac{\partial u_s}{\partial x}) + \frac{\partial}{\partial y} (v_t \frac{\partial u_s}{\partial y}) + \\ & - \frac{\tau_{bp_x}}{\rho h} - \frac{\tau_{bs_x}}{\rho h} - \frac{1}{\rho h} (\frac{\partial S_{xx}}{\partial x} + \frac{\partial S_{xy}}{\partial y}) + \frac{W_x}{\rho h} \end{aligned} \quad (12)$$

in which τ_{bp_x} and τ_{bs_x} are the bottom shear stress components related to the primary and the secondary flow, respectively, and W_x is the x-component of the wind shear stress at the water surface. S_{xx} and S_{xy} are components of the radiation stress.

Elimination of the pressure gradient term from (11) and (12) leads to an equation that can be elaborated to

$$\begin{aligned} & \frac{\partial}{\partial z} (v_t \frac{\partial u_p}{\partial z}) + \frac{\tau_{bp_x}}{\rho h} + \frac{\partial}{\partial z} (v_t \frac{\partial u_s}{\partial z}) + \frac{\tau_{bs_x}}{\rho h} + f_c v_s = \\ & \frac{W_x}{\rho h} + \frac{\partial}{\partial x} (\langle \tilde{u}^2 \rangle - \langle \tilde{w}^2 \rangle) - \frac{1}{\rho h} \frac{\partial S_{xx}}{\partial x} + \frac{\partial}{\partial y} (\langle \tilde{u}\tilde{v} \rangle) - \frac{1}{\rho h} \frac{\partial S_{xy}}{\partial y} + \\ & + (f_p - 1) (\frac{\partial \bar{u}}{\partial t} - f_c \bar{v}) + (f_p^2 - f_s^2) (\bar{u} \frac{\partial \bar{u}}{\partial x} + \bar{v} \frac{\partial \bar{u}}{\partial y}) + \text{other terms} \end{aligned} \quad (13)$$

The "other terms" in this equation concern the vertical non-uniformity of the advection of secondary flow momentum by the primary and the secondary current, the advection of primary flow momentum by the secondary

current and the horizontal diffusion of primary and secondary flow momentum. For the time being, all these terms will be disregarded.

From Eq. (13) a further specification of the primary and the secondary current is possible. The **primary current** is defined such, that

$$\frac{\partial}{\partial z} \left(\nu \frac{\partial u_p}{\partial z} \right) + \frac{\tau_{bp_x}}{\rho h} = 0 \quad (14)$$

The direction of the primary bottom shear stress is assumed to coincide with the depth-averaged flow direction. Hence eq. (14) describes the vertical distribution function of the primary flow and establishes the relationship between the primary bottom shear stress and the depth-averaged velocity. This makes the y-equivalent of this equation redundant. Since the turbulence viscosity is given a vertical distribution and its depth-average is related to the current and wave properties, the primary flow velocity and associated bottom shear stress can be determined. The evaluation by DVS leads to a primary flow model, consisting of a profile function, a bottom shear stress relationship and the conventional depth-integrated equations.

For the **secondary flow** the following equation may be derived after substitution of (14) into (13).

$$\begin{aligned} \frac{\partial}{\partial z} \left(\nu \frac{\partial u_s}{\partial z} \right) + \frac{\tau_{bs_x}}{\rho h} + f_c v_s = \\ \frac{W_x}{\rho h} + \frac{\partial}{\partial x} \langle \tilde{u}^2 \rangle - \langle \tilde{w}^2 \rangle - \frac{1}{\rho h} \frac{\partial S_{xx}}{\partial x} + \frac{\partial}{\partial y} \langle \tilde{u}\tilde{v} \rangle - \frac{1}{\rho h} \frac{\partial S_{xy}}{\partial y} + \\ (f_p - 1) \left(\frac{\partial \bar{u}}{\partial t} - f_c \bar{v} \right) + (f_p^2 - \bar{f}_p^2) \left(\bar{u} \frac{\partial \bar{u}}{\partial x} + \bar{v} \frac{\partial \bar{u}}{\partial y} \right) \end{aligned} \quad (15)$$

According to this equation, there are four sources of secondary flow, viz.

- the wind shear stress at the water surface, which gives rise to a current velocity with a vertical distribution that deviates from the primary current distribution and, if the coriolis-effect is important, even to a velocity direction that varies along the vertical (Ekman, 1905)
- the vertical non-uniformity of the wave-induced forces, related to the mass flux above the wave through level and the returnflow or undertow below this level (Dyhr-Nielsen and Sørensen, 1970)
- the vertical non-uniformity of the main flow acceleration, in time and due to the coriolis-effect (also see Kalkwijk and Booij, 1986)
- the vertical non-uniformity of the advective accelerations of the main flow, including the well-known curvature-induced secondary flow (Boussinesq, 1868), but also the deformation of the current profile due to downstream accelerations.

In complex coastal areas, each of these secondary currents can have an important effect on the morphological evolution. Therefore, each of them deserves full attention when developing a mathematical model of coastal morphology. Practical restrictions, however, allowed DVS to evaluate only one of them, viz. the wave-induced secondary flow. In fact, this means that they focussed their attention on the surf zone of a nearly

uniform coast, although their formulations are so general, that they basically allow for more complex situations.

3. WAVE-INDUCED SECONDARY CURRENT

In order to describe the wave-induced secondary current, DVS divide the water column in three layers: a surface layer above wave trough level, a middle layer, and a bottom layer. Following Stive and Wind (1986) the surface layer is accounted for via an effective shear stress at trough level, compensating for the momentum decay above it.

The velocity in the bottom layer can contribute substantially to the total sediment transport. Because of the natural irregularity of a mobile bottom, however, DVS argue that a detailed description of this velocity hardly makes sense, unless it is needed to assess the influence on the velocity in the middle layer. Therefore, the bottom layer velocity due to non-breaking waves is assumed to be similar to Longuet-Higgins' (1953) conduction solution. For breaking waves, Stive and Wind (1986) show that assuming a zero bottom shear stress leads to acceptable predictions of the secondary current outside the wave boundary layer. So, in the initial formulation of the quasi-3D model the bottom layer was left out of consideration for this part of the current. As a next step the velocity in the middle layer is solved, both for the breaking and the non-breaking fraction of the waves. In either cases a prescribed shear stress at the trough level provides an upper boundary condition, whereas the lower boundary condition follows from the zero shear stress approximation (breaking waves) or from matching with the bottom layer solution (non-breaking waves).

The above treatment of the wave boundary layer flow is rather inconsistent where it concerns the breaking wave situation. Recently, Svendsen et al. (1987) proposed an approach which solves the boundary layer flow under breaking waves. On the basis of the horizontal momentum balance for the boundary layer a solution was sought, which uses boundary conditions based on patching the flow between middle and bottom layer. This method of patching is used in the following evaluation of the three-layer approach, so that the relevance of this method for the quasi-3D model can be determined. It is noted that in the following - as in DVS - we consider a random wave field with breaking and non-breaking wave fractions, between which we assume no interaction, so that their respective contributions to the secondary current may be superimposed. Being specifically interested in the secondary flow we restrict our attention to the case of waves normally incident to the coast.

The **surface layer** is accounted for via the effective shear stress at trough level, which compensates for the momentum decay above it. Following DVS it is the sum of viscous dissipation at the surface in non-breaking waves and the momentum loss above the wave trough level due to breaking.

$$\tau(t) = \rho \nu_t \frac{\tilde{u}_b^2 k}{c} \sinh(2kh) + \left(\frac{1}{2} + \frac{7kh}{2\pi}\right) \frac{D}{c} \quad (16)$$

where ν_t is the kinematic viscosity,
 k the wave number,
 c the wave phase speed,

D the mean energy dissipation due to wave breaking,
 \tilde{u}_b the near-bottom oscillatory velocity amplitude.

The other integral property of the surface layer is its mean mass flux m which DVS estimate at

$$m = \left(1 + \tilde{Q}_b \frac{7kh}{2\pi}\right) \frac{E}{c} \quad (17)$$

where \tilde{Q}_b is the breaking wave fraction and
 E is the mean energy density of the wave field.

In the **middle layer** the prevailing local horizontal mean momentum balance in cross-shore direction reads:

$$\frac{\partial}{\partial z} \left(v_t \frac{\partial U}{\partial z} \right) = \frac{\partial}{\partial x} \left(\langle \tilde{u}^2 \rangle - \langle \tilde{w}^2 \rangle \right) + g \frac{\partial \langle z_s \rangle}{\partial x} \quad (18)$$

where U is now the only secondary flow component present, induced by the waves in cross-shore direction, and $\partial \langle z_s \rangle / \partial x$ is the only pressure gradient term present, due to the set-down/set-up. For simplicity we introduce

$$\alpha(x, z) = \frac{\partial}{\partial x} \left(\langle \tilde{u}^2 \rangle - \langle \tilde{w}^2 \rangle \right) + g \frac{\partial \langle z_s \rangle}{\partial x} \quad (19)$$

In the **bottom boundary layer** there is an additional term in the prevailing momentum balance equation, viz. the wave-induced Reynolds stress:

$$\frac{\partial}{\partial z} \left(v_{tb} \frac{\partial U}{\partial z} \right) = \alpha + \frac{\partial}{\partial z} \left(\langle \tilde{u} \tilde{w} \rangle \right) \quad (20)$$

The boundary conditions for the above momentum equations are

- the shear stress condition at trough level

$$v_t \frac{\partial U}{\partial z} = \frac{\tau(t)}{\rho} \text{ at } z = z_t;$$

- the patching conditions at the top of the bottom boundary layer, requiring continuity in U and τ at $z = z_\ell$;
- the no-slip condition at the bottom: $U = 0$ at $z = z_b$

In addition, we have the integral condition of continuity, which for the two lower layers reduces to

$$\int_{z_b}^{z_t} U dz = - m / \rho \quad (21)$$

In order to solve the above set of equations and boundary conditions we need to specify the turbulence viscosity distribution. For simplicity we adopt a uniform distribution in both the bottom and the middle layer, where - following Svendsen et al. (1987) - the bottom layer value is several orders of magnitude smaller (for the middle layer see DVS):

$$\begin{aligned} v_{tb} &= c_f^2 \frac{\tilde{u}_b^2}{\omega} & \text{for } z < z_\ell \\ v_t &= M h \left(\frac{D}{\rho} \right)^{1/3} & \text{for } z > z_\ell \end{aligned} \quad (22)$$

Furthermore, we adopt the finding of Stive and Wind (1986) that α is virtually constant over depth:

$$\alpha(x, z) \approx \alpha(x) \quad (23)$$

Solution procedure

Taking account of the shear stress condition at trough level, the solution for the middle layer momentum balance reads:

$$U = U(z_\ell) + \frac{\tau(t)}{\rho v_t} (z - z_\ell) - \frac{\alpha}{v_t} \left[\frac{1}{2} (z_\ell - z_t)^2 - \frac{1}{2} (z - z_t)^2 \right] \quad (24)$$

in which $U(z_\ell)$ and α are still unknown.

Taking account of the no-slip condition at the bottom, the solution for the bottom layer reads:

$$U = \frac{\tau(b)}{\rho v_{tb}} (z - z_b) + \frac{\alpha}{v_{tb}} \frac{1}{2} (z - z_b)^2 + U_s(z) \quad (25)$$

where U_s is the conduction solution for the wave-induced flow in the absence of a pressure gradient (Longuet-Higgins, 1953). In equation (25) τ_b and α are still unknown.

Patching the velocities and the shear stresses at $z = z_\ell$ yields

$$U(z_\ell) = \frac{\tau(b)}{\rho v_{tb}} (z_\ell - z_b) + \frac{\alpha}{v_{tb}} \frac{1}{2} (z_\ell - z_b)^2 + U_s(z_\ell) \quad (26)$$

and

$$\frac{\tau(b)}{\rho} = \frac{\tau(t)}{\rho} - \alpha (z_t - z_b) - \overline{\tilde{u} \tilde{w}}|_{z_\ell} \quad (27)$$

Finally, the integral condition of continuity requires:

$$\int_{z_\ell}^{z_t} (\text{eq. 24}) dz + \int_{z_b}^{z_\ell} (\text{eq. 25}) dz = -m/\rho \quad (28)$$

The unknowns $U(z_\ell)$, $\tau(b)$ and α can be solved from equations (26) through (28); e.g. for α we can derive:

$$\begin{aligned} \alpha \left[\frac{1}{3} \frac{(d_t - \delta)^2}{v_t} + \frac{d_t \delta (d_t - \delta)}{v_{tb}} - \frac{1}{2} \frac{\delta^2 (d_t - \delta)}{v_{tb}} + \frac{1}{2} \frac{d_t \delta^2}{v_{tb}} - \frac{1}{6} \frac{\delta^3}{v_{tb}} \right] = \\ \frac{\tau(t)}{\rho} \left[\frac{1}{3} \frac{(d_t - \delta)^2}{v_t} + \frac{\delta (d_t - \delta)}{v_{tb}} + \frac{1}{2} \frac{\delta^2}{v_{tb}} \right] - \overline{\tilde{u} \tilde{w}}|_{z_\ell} \left[\frac{\delta (d_t - \delta)}{v_{tb}} + \frac{1}{2} \frac{\delta^2}{v_{tb}} \right] + \\ + U_s(z_\ell) [(d_t - \delta) + \frac{1}{2} \delta] + m/\rho, \end{aligned} \quad (29)$$

where $d_t \hat{=} z_t - z_b$,

$\delta \hat{=} z_\ell - z_b$,

$$\text{and } \overline{\tilde{u} \tilde{w}}|_{z_\ell} = \frac{1}{2} k \tilde{u}_b^2 \delta [e^{-1}(\sin(1) + \cos(1)) - \frac{1}{2} e^{-2} - \frac{1}{2}] \quad (30)$$

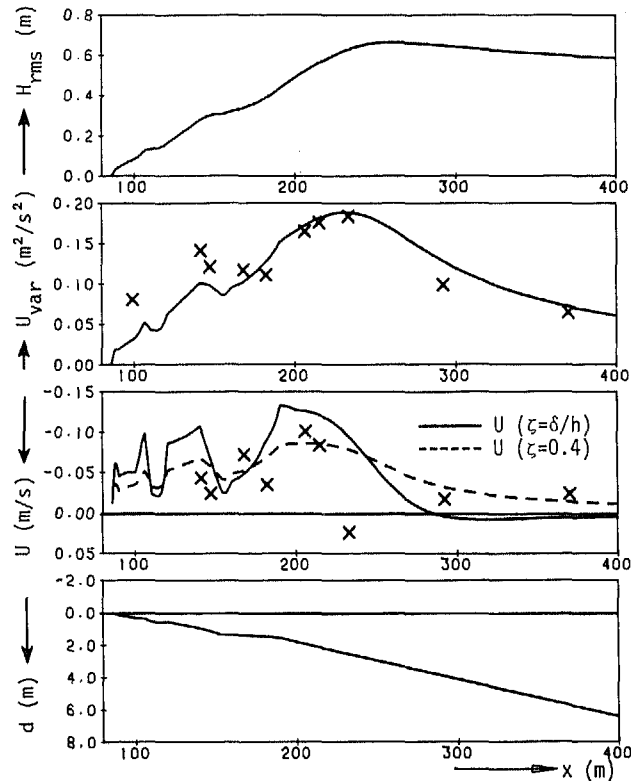


Fig. 1 Results (after DVS) for NSTS conditions Nov. 20, 1978 at Torrey Pines beach (measurements after Guza and Thornton, 1985); profile of bottom elevation below MSL (d), cross-shore current (U), variance of horizontal orbital velocity (u_{var}) and rms wave height (H_{rms}) versus distance normal to shore (x). Data points: measured values. Curves: computational results.

$$U_s(z_b) = \frac{\tilde{u}_b^2}{c} [3 + e^{-2} - 2e^{-1}(3\cos(1))]. \quad (31)$$

Finally, it is noted that the conditions imposed here determine the solution exactly and uniquely. The depth-integrated momentum equation is consistent with this solution and adds no new information to the system. If, nevertheless, this latter equation is used, e.g. to determine the mean surface slope $\partial\langle z_g \rangle / \partial x$ (and thus α), one of the other conditions should be dropped.

Results

In discussing results from the above formulations two aspects are distinguished. Firstly, the secondary flow distribution as such is investigated; its sensitivity for important parameters is analyzed and a comparison is made with the results obtained by DVS. The second aspect concerns the bottom shear stress due to the secondary current; from the

present results it is possible to check whether neglecting this shear stress - as in DVS - is justified. The following presentation is restricted to the conditions during an NSTS campaign at Torrey Pines after Guza and Thornton (1985). This campaign has yielded one of the few field data sets known to the authors suitable for the present purposes. The comparison of DVS of their theoretical results and these field measurements (see Figure 1) gives a general indication to which level we are able to check the accuracy of the secondary flow results.

Results for the secondary current from the present formulation at two characteristic elevations, viz. at the top of the bottom layer and at 0.4 times the water depth, are given in Figure 2. In addition to a comparison with the formulation of DVS, results are given for a different setting of the parameters that are not well known and to which the model results are expected to be sensitive. These concern the patching height δ and the friction coefficient c_f ; the latter determines the thickness of the oscillatory wave boundary layer δ_w and the turbulence viscosity in the bottom layer.

The initial parameter setting was chosen as realistic as possible, with the patching level at the edge of the oscillatory wave boundary layer, $\delta = \delta_w$, and the friction coefficient based on the sediments grain roughness, $c_f = 0.01$. The sensitivity of the results for these parameters is investigated by taking the patching height at twice the boundary layer thickness above the fixed bed in one case and by taking $c_f = 0.02$, implying a roughness increase by an order of magnitude, in the other case.

Inspection of the various results in Figure 2 leads to the conclusion that at these levels the difference between the present formulation and that of DVS is not significant compared with the sensitivity of the present formulation to the patching height and the friction coefficient. The near bottom secondary current velocity is apparently the most sensitive quantity, but a comparison with the available measured data, yields no definitive conclusions.

A more detailed comparison between the present and DVS's formulation for the initial parameter setting involving the full vertical distribution of the secondary current is given in Figure 3 for two specific locations, viz. at $x = 190$ m, approximately the location with a maximum in the energy dissipation, and at $x = 105$ m, a location where virtually all waves are breaking. As expected from the above results, the differences above the bottom layer are small. Of course, only the present model can be realistic close to the bottom, since it takes account of the no-slip condition at the fixed bed level.

The other set of results, with a possible impact on the sediment transport, concerns the bottom shear stress due to the secondary current. Results for the bottom shear stress and related terms from Equation (27) are presented in Figure 4.

It appears that the bottom shear stress $\tau(b)$ closely corresponds with the difference between the set-up dominated term $\rho \alpha d$ and the radiation stress decay dominated term $\tau(t)$. The maximum actual difference is approximately 20%. The effect in the total set-up is a few percent only, so that the usual neglect of the bottom shear stress in e.g. the depth-averaged cross-shore momentum balance is justified.

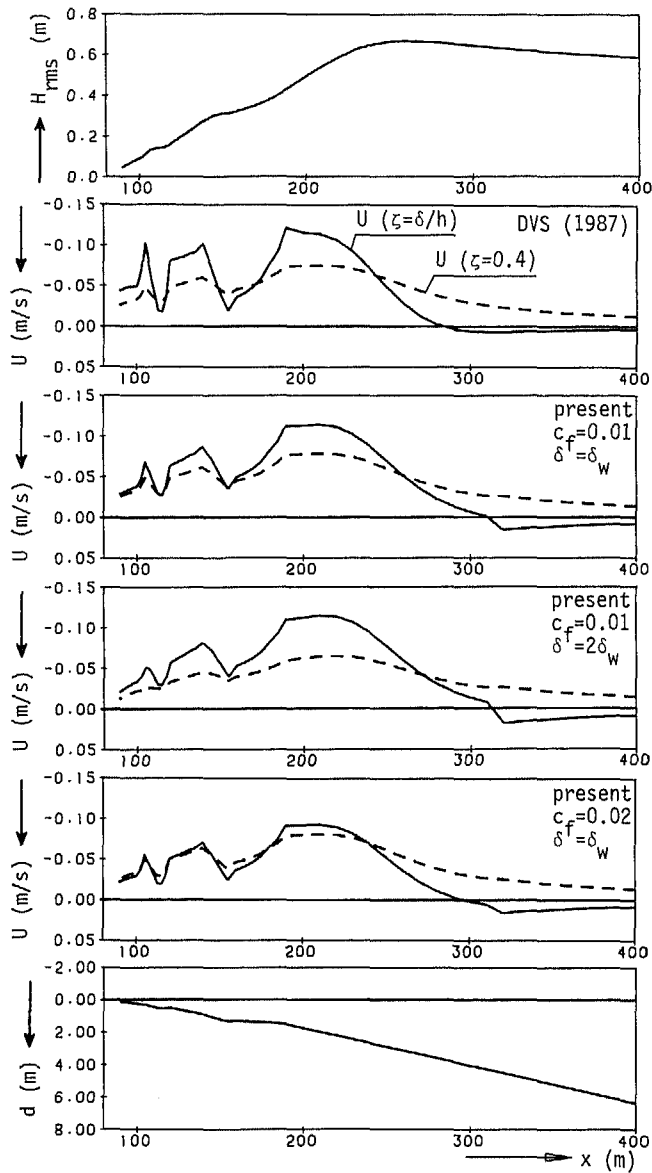


Fig. 2 Results for NSTS conditions Nov. 20, 1978 at Torrey Pines beach; profile of bottom elevation below MSL (d), cross-shore current (U) for DVS and present model and rms wave height (H_{rms}) versus distance normal to shore (x).

However, the impact on the mean bottom shear stress direction in a uniform longshore current situation may be larger, since even a small secondary bottom shear stress will cause a deviation from the longshore direction due to its large angle with the primary shear stress direction.

As an example, let us consider a wave-induced longshore current along a uniform beach. The primary bottom shear stress is given by

$$\tau_p(b) \approx \frac{D}{c} \sin\theta \quad (32)$$

where θ is the angle of wave incidence with the shore normal x -direction (positive shoreward). According to the above findings the secondary bottom shear stress amounts some 10% of the trough shear stress

$$\tau_s(b) \approx 0.1 \tau(t) \approx (0.05 + 0.7 \frac{kh}{2\pi}) \frac{D}{c} \quad (33)$$

With $kh = 0.2$ as a typical value the angle α^1 of the total shear stress vector with the shore normal follows from

$$\tan \alpha^1 = \frac{\tau_p(b) + \tau_s(b) \sin\theta}{\tau_s(b) \cos\theta} \approx \frac{1-0.07}{-0.07} \tan\theta \quad (34)$$

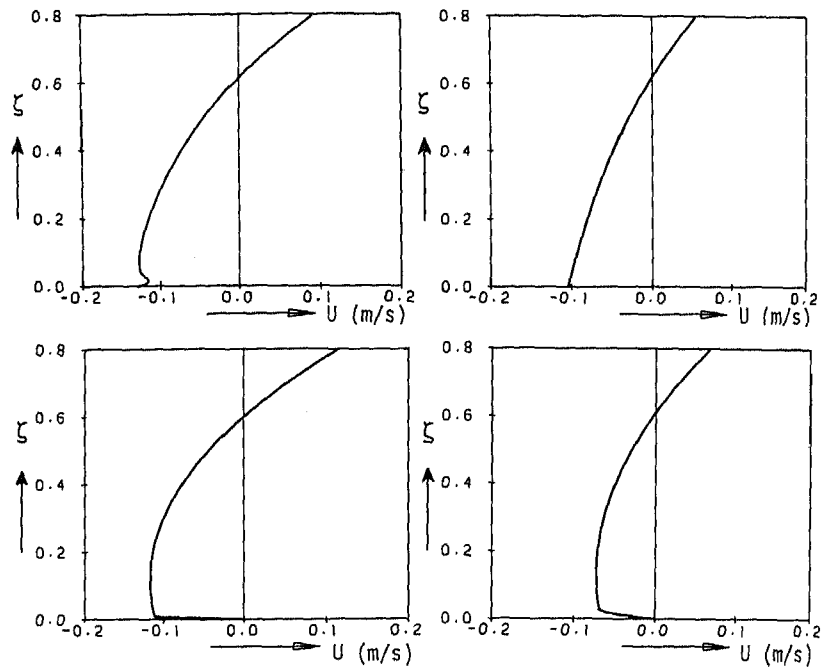


Fig. 3 Vertical distributions of the wave-induced secondary (cross-shore) current according to DVS (top) and present model (bottom; $c_f = 0.01$, $\delta = \delta_0$) for NSTS conditions Nov. 20, 1978 at Torrey Pines beach. at $x = 190$ m (left) and $x = 150$ m (right).

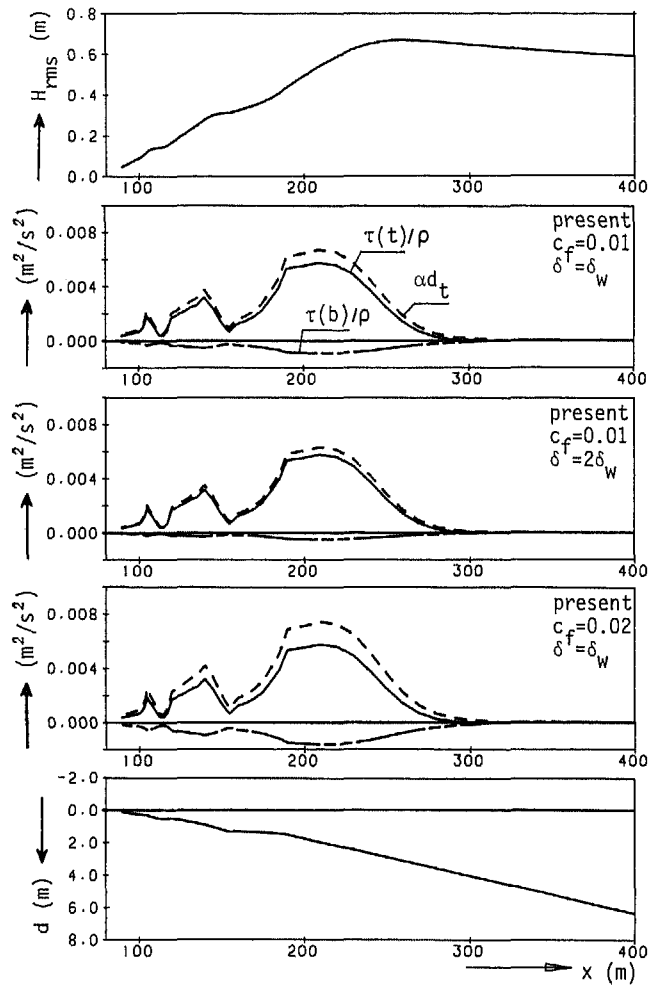


Fig. 4 Results for NSTS condition Nov. 20, 1978 at Torrey Pines beach; profile of bottom elevation below MSL (d), shear stress at trough ($\tau(t)$) and bottom level ($\tau(b)$) and local radiation stress gradient (αd_t), and rms wave height (H_{rms}) versus distance normal to shore (x).

For wave incidence angles of 5° and 30° , we then find that the deviation angle of the total shear stress vector from the alongshore direction is 49° and 83° seawards, respectively. Obviously, these figures are important when defining bottom boundary conditions for nearshore sediment transport computations.

4. CONCLUSIONS

In a quasi-3D nearshore current model the wave-induced secondary current distribution above the bottom boundary layer may well be predicted from a three layer approach in which the surface layer is accounted for by an effective shear stress and a mass flux condition and in which the dynamics of the bottom layer are virtually neglected. However, a realistic distribution of the wave-induced secondary current close to the bottom, can only be found if the bottom layer dynamics are taken into account via a momentum balance which includes the set-up induced pressure gradient, e.g. following the approach suggested by Svendsen et al. (1987). Furthermore, it appears that the secondary bottom shear stress in the latter case can cause a substantial deviation of the total shear stress direction from the alongshore direction. Hence it cannot be disregarded in sediment transport computations.

ACKNOWLEDGEMENT

The present study was carried out as a part of TOW Coastal Research Program, which is financed by Rijkswaterstaat of the Ministry of Transport and Public Works of the Netherlands. The authors wish to thank Prof. I.A. Svendsen for sending draft publications and for his stimulating discussions.

REFERENCES

- Berkhoff, J.C.W., 1976. Mathematical models for simple harmonic linear water waves; wave diffraction and refraction. Doct. thesis, Delft Univ. of Techn., 103 pp. (also: Delft Hydr. Lab., Publ. no.163).
- Boussinesq, J., 1968. Mémoire sur l'influence de frottement dans les mouvements réguliers des fluides. J. de Math.Pures et Appl., 2ème Série, Tome XIII, p.413
- Davies, A.M., 1980. Application of the Galerkin-method to the formulation of a three-dimensional nonlinear hydrodynamic numerical sea-model. Appl. Meth. Mod., 4, no. 4, p. 245-256.
- De Vriend, H.J., 1981. Steady flow in shallow channel bends. Doct. thesis Delft Univ. of Techn., 260 pp. (also: Dept. of Civil Engrg., Comm. on Hydraulics, no. 81-3).
- De Vriend, H.J. and Stive, M.J.F., 1987. Quasi-3D modelling of nearshore currents. JONSMOD'86, Delft, The Netherlands (accepted for publication in JONSMOD-issue of Coastal Eng.).
- Dyhr-Nielsen, M. and Sørensen, T., 1970. Some sand transport phenomena on coasts with bars. Proc. 12th ICCE, Washington, p. 855-865.
- Ekman, V.W., 1905. On the influence of the earth's rotation on ocean currents. Ark.f.Mat., Astron. och Fysik, 2, 11, p. 1-53.
- Guza, R.T. and Thornton, E.B., 1985. Velocity moments in nearshore. Waterway, Port, Coastal and Ocean Engrg., 111, no.2, p. 235-256.
- Kalkwijk, J.P.Th. and Booij, R., 1986. Adaptation of secondary flow in nearly-horizontal flow. Hydr. Res., 24, 1, p. 19-37.
- Longuet-Higgins, M.S., 1953. Mass transport in water waves. Phil.Trans. Royal Soc., A254, p. 535-581.
- Stive, M.J.F., and Wind, H.G., 1986. Cross-shore mean flow in the surf zone. Coastal Engineering, 10 (1986), p. 325-340.
- Svendsen, I.A., Schäffer, H.A. and Buhr Hansen, J., 1987. The interaction between the undertow and the boundary layer flow on a beach. Submitted for publication.